This article has been accepted for publication in 2022 IEEE International Symposium on Personal, Indoor and Mobile Radio Communications. This is the author's version which has not been fully edited and content may change prior to final publication.
Link to the published version: DOI: 10.1109/PIMRC54779.2022.9977686

Distributed Cooperative Transmission in MANETs with Multiple Timing and Carrier Frequency Offsets

Mus'ab Yüksel
Hochschule Darmstadt
Darmstadt, Germany
musab.yueksel@h-da.de

Raphael T. L. Rolny
armasuisse Science and Technology
Thun, Switzerland
raphael.rolny@armasuisse.ch

Marc Kuhn
ZHAW
Winterthur, Switzerland
kumn@zhaw.ch

Michael Kuhn
Hochschule Darmstadt
Darmstadt, Germany
michael.kuhn@h-da.de

***Abstract*—Cooperative transmission is a promising approach to establish robust communication in Mobile Ad-Hoc Networks (MANETs). In low-complexity MANETs several transmitters (TX) can be aggregated to a virtual multiple input system. For such a setup, the impact of various timing and carrier frequency offsets (TO, CFO) has to be mitigated. We propose an effective, purely time-domain based equalizer structure that allows to establish cooperative transmission with a transmit diversity scheme in presence of aforementioned impairments and multipath channels. Exemplarily investigating the broadcast performance by outage simulations in a MANET scenario, we can demonstrate the benefits and indicate that the proposed structure is auspicious to improve the general scalability of MANETs.**

***Index Terms*—MANET Scalability, Distributed Cooperative Transmission (Broadcasting), Space-Time Block Codes (STBC), Carrier Frequency Offset (CFO), Timing Offset (TO)**

I. Challenges in High Mobility Scenarios

Mobile Ad-Hoc Networks (MANETs) are infrastructure-less and typically consist of low-power, low-cost, low-complexity nodes [1]. Cooperative transmission, i. e. the simultaneous transmission with several nodes, is a promising approach to establish a more robust communication that can pave the way towards an overall improved scalability [2]. In a typical MANET as depicted in Fig. 1 several imperfections have to be expected. Each node, equipped with an own oscillator introduces a varying carrier frequency offset (CFO), whereas mobility generates additional CFO due to the Doppler shift. Since the nodes are located at a different distance to each other, the propagation time varies raising a timing offset (TO), while imperfect synchronization among the nodes is a further source for TO. Besides, particularly for high-rate transmissions, multipath propagation is prevalent provoking a channel delay spread. High node mobility reinforces the aforementioned effects.

Multipath propagation and TO originate inter-symbol-interference (ISI), whereas CFO causes a non-perfect alignment of the transmit signals in the frequency domain which can result in a severely degraded performance if not mitigated. The impact of impairments is a major problem that has been widely discussed in literature. Nevertheless, proposed schemes either concentrate on a rather low number of transmitting nodes, i. e. systems with a dedicated size [3] or introduce a rate loss [4], [5]. Besides, they presuppose quasi-static narrow-band channels [6], [7] or require a guard interval between two adjacent blocks to avoid interference [3], [8]. Often an exhaustive maximum likelihood decoding is foreseen, which is no longer feasible for an increased block length or number of transmitters (TX) [9]. Proposed low-complexity alternatives come at the downside of a majorly degraded performance for large block lengths [10]. Some schemes loose their properties once a TX signal is in deep fade, which however will very likely happen in a fading environment [6]. A few schemes require exact knowledge about the location of each node at the RX [4] or are based on a feedback link [5].

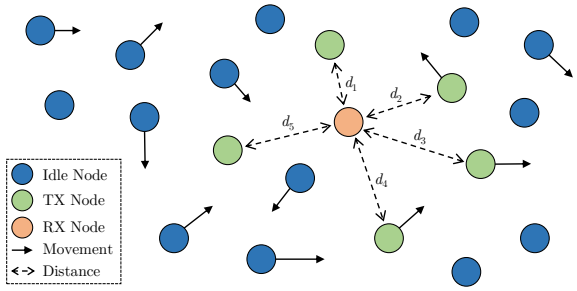

Fig. 1. MANET system model: distributed nodes each with a different oscillator, moving direction, velocity and distance to other nodes

In general, multi-carrier schemes, such as OFDM or SC-FDMA, are known to be well-suited to overcome multipath propagation and multiple TO by employing an appropriately designed cyclic prefix (CP). Nevertheless, multiple CFO will cause inter-carrier-interference (ICI) whose compensation is not straightforward. Employing a classical single-carrier scheme allows a time-domain equalization, besides being computationally more efficient as no Fourier transformation is required. Furthermore, the CP and the common use of guard carriers actually constitute a rate loss, which can be avoided by a sophisticated single-carrier design.

Therefore, we propose an efficient equalizer structure for a single-carrier transmit diversity scheme that enables cooperative transmission for distributed nodes in presence of aforementioned impairments. For that, we utilize inherent code properties of Linear-Scalable Dispersion Codes (LSDCs) [11]. Our proposed equalizer allows a cooperative transmission that

- supports an arbitrary number of TX,
- does not require a feedback link or knowledge about the

nodes' position,
- is capable to deal with multipath channels,
- achieves full transmit diversity and rate one with an efficient suboptimal decoder,
- allows for a concatenation of blocks without the need for a guard interval,
- is robust against transmitters in deep fade,
- is robust against arbitrary multiple (integer and fractional) delays,
- is robust against arbitrary multiple carrier frequency offsets at the same time.

To demonstrate the effectiveness of the proposed equalizer and cooperative transmission, we investigate the broadcasting performance for MANETs with varying population sizes. *Notation:* x denotes a scalar, $\mathbf{x}$ a vector, $\mathbf{X}$ a matrix and $\ddot{\mathbf{X}}$ a diagonal matrix where $\mathbf{X}(i,j) = 0$ for $i \neq j$. $(\cdot)^H$ refers to the adjoint (complex transpose) and $(\cdot)_\mathrm{i}$ to a node specific description.

II. Transmit Diversity Scheme: Impacts of Imperfections

Space-Time Block-Codes (STBCs) initially designed as transmit diversity schemes for co-located antennas at one node can be adapted to establish cooperative transmission for distributed nodes [2]. We focus only on linear codes, as non-linear, e. g. trellis based codes can become computationally expensive for large block lengths. Linear codes themselves can in turn be subdivided into several families. However, those that are based on an orthogonal or quasi-orthogonal structure are not suited for distributed cooperative transmission in MANETs, as imperfections will have a significant impact on the orthogonality leading to a tremendously degraded performance. In contrast, LSDCs are promising, as they rely on ISI, that is artificially introduced to achieve the best-possible transmit diversity gain. Fundamentally, LSDCs employ two linear codes that are decoupled. The time invariant outer code $\mathbf{R} \in \mathbb{C}^{N_\mathrm{C},N_\mathrm{I}}$, where N_C denotes the block length and N_I the number of input symbols, is optimized to achieve the best-possible transmit diversity. The time variant (denoted by the index ν) inner code $\mathbf{C}_\nu \in \mathbb{C}^{N_\mathrm{C},N_\mathrm{TX}}$, where N_TX refers to the number of transmitters, is designed for channel adaptation. At the receiver (RX) the overall matched received symbol $\mathbf{y}_\mathrm{m}$ can be obtained by

$$\mathbf{y}_\mathrm{m} = \mathbf{R}^H \cdot \ddot{\mathbf{D}} \cdot \mathbf{R} \cdot \boldsymbol{\alpha} + \mathbf{n} = \boldsymbol{\Lambda} \cdot \boldsymbol{\alpha} + \mathbf{n}, \tag{1}$$

where $\boldsymbol{\alpha} \in \mathbb{C}^{N_\mathrm{I},1}$ refers to the input symbol vector and $\mathbf{n} \in \mathcal{CN}\left(0, \sigma_\mathrm{n}^2 \mathbf{I}\right)$ to the complex-valued additive white Gaussian noise (AWGN). $\ddot{\mathbf{D}} \in \mathbb{C}^{N_\mathrm{C},N_\mathrm{C}}$ is a diagonal matrix that summarizes the impact of the channel as well as the inner code. This initial design for co-located antennas does neither consider multipath propagation, nor timing or carrier frequency offset. Regarding the encoding for distributed nodes, each node i uses a different inner code $\ddot{\mathbf{C}}_{\mathrm{TX,i}} \in \mathbb{C}^{N_\mathrm{C},N_\mathrm{C}}$ to calculate its specific transmit signal $\mathbf{u}_\mathrm{i} \in \mathbb{C}^{N_\mathrm{C},1}$ as

$$\mathbf{u}_\mathrm{i} = \ddot{\mathbf{C}}_{\mathrm{TX,i}} \cdot \boldsymbol{\alpha}_\mathrm{TX} = \ddot{\mathbf{C}}_{\mathrm{TX,i}} \cdot \mathbf{R} \cdot \boldsymbol{\alpha}, \tag{2}$$

where $\ddot{\mathbf{C}}_{\mathrm{TX,i}}$ denotes a diagonal matrix whose elements correspond to one column of the inner code matrix $\mathbf{C}_\nu$.
In general, a different complex multipath channel has to be assumed for each link between the i-th TX and RX. Hence, the corresponding channel vector $\mathbf{h}_{\mathrm{TX,i}} \in \mathbb{C}^{N_\mathrm{taps},1}$ consists of at least one non-zero complex channel coefficient. For each link, the impact of the channel can be described by a linear convolution as

$$\mathbf{u}_{\mathrm{ch,i}} = \mathbf{u}_\mathrm{i} * \mathbf{h}^\Theta_{\mathrm{TX,i}} + \mathbf{n} = \mathbf{H}^\Theta_{\mathrm{TX,i}} \cdot \mathbf{u}_\mathrm{i} + \mathbf{n}. \tag{3}$$

τ_i denotes the propagation delay in samples between the i-th TX and RX and $\mathbf{H}_{\mathrm{TX,i}} \in \mathbb{C}^{N_\mathrm{C}+N_\mathrm{taps}-1,N_\mathrm{C}}$ the corresponding convolution matrix, i. e. a Toeplitz matrix generated by $\mathbf{h}_{\mathrm{TX,i}}$. While $N_\mathrm{taps} \cdot t_\mathrm{s}$ constitutes the channel delay spread, where t_s refers to the system's sample time, the propagation delay can be modelled by prepending zeros to $\mathbf{h}_{\mathrm{TX,i}}$, so that $\mathbf{h}^\Theta_{\mathrm{TX,i}} \in \mathbb{C}^{\tau_\mathrm{i}+N_\mathrm{taps},1}$. Accordingly, the corresponding convolution matrix $\mathbf{H}^\Theta_{\mathrm{TX,i}} \in \mathbb{C}^{N_\mathrm{C}+N_\mathrm{taps}+\tau_\mathrm{i}-1,N_\mathrm{C}}$ that respects the link specific delay τ_i is a Toeplitz matrix generated by $\mathbf{h}^\Theta_{\mathrm{TX,i}}$.
Additionally, multiple CFO has to be considered, which results from the mismatch between the oscillators of each TX and RX. In general, the CFO is different for each node, whereas we assume that it is constant for at least one encoded block. Prior to the superposition of the intermediate signals $\mathbf{u}_{\mathrm{ch,i}} \in \mathbb{C}^{N_\mathrm{C}+N_\mathrm{taps}+\tau_\mathrm{i}-1,1}$ the impact of CFO can be considered by a multiplication with a diagonal matrix $\dddot{\mathbf{\Phi}}_{\mathrm{TX,i}} \in \mathbb{C}^{N_\mathrm{C}+N_\mathrm{taps}+\tau_\mathrm{i}-1,N_\mathrm{C}+N_\mathrm{taps}+\tau_\mathrm{i}-1}$ where the ν-th diagonal element corresponding to the ν-th time-slot can be expressed by

$$\dddot{\mathbf{\Phi}}_{\mathrm{TX,i}}(\nu,\nu) = \mathrm{e}^{j \cdot 2\pi \cdot \mathrm{CFO_i} \cdot \nu \cdot t_\mathrm{s}} = \phi_\mathrm{i}^\nu, \tag{4}$$

so that

$$\dddot{\mathbf{\Phi}}_{\mathrm{TX,i}} = \begin{pmatrix} \phi_\mathrm{i}^0 & 0 & \dots & \dots & 0 \\ 0 & \phi_\mathrm{i}^1 & 0 & \dots & 0 \\ \vdots & 0 & \ddots & 0 & 0 \\ \vdots & \vdots & \vdots & \ddots & 0 \\ 0 & 0 & 0 & 0 & \phi_\mathrm{i}^{N_\mathrm{C}+N_\mathrm{taps}+\tau_\mathrm{i}-2} \end{pmatrix}, \tag{5}$$

where $\mathrm{CFO_i}$ refers to the CFO of the i-th TX. With that (3) finally becomes

$$\mathbf{u}_{\mathrm{ch,i}} = \dddot{\mathbf{\Phi}}_{\mathrm{TX,i}} \cdot \mathbf{H}^\Theta_{\mathrm{TX,i}} \cdot \mathbf{u}_\mathrm{i} + \dddot{\mathbf{\Phi}}_{\mathrm{TX,i}} \cdot \mathbf{n}, \tag{6}$$

so that the received symbol vector $\mathbf{y}$ can be denoted as

$$\mathbf{y} = \sum_{i=1}^{N_\mathrm{TX}} \mathbf{u}_{\mathrm{ch,i}} = \sum_{i=1}^{N_\mathrm{TX}} \dddot{\mathbf{\Phi}}_{\mathrm{TX,i}} \cdot \mathbf{H}^\Theta_{\mathrm{TX,i}} \cdot \mathbf{u}_\mathrm{i} + \dddot{\mathbf{\Phi}}_{\mathrm{TX,i}} \cdot \mathbf{n}. \tag{7}$$

III. Proposed Equalizer Architecture

To mitigate the impact of imperfections, we generate an appropriate correlation matrix $\boldsymbol{\Lambda}$ that can be written as

$$\boldsymbol{\Lambda} = \mathbf{R}^H \cdot \boldsymbol{\Lambda}_\mathrm{Q} \cdot \mathbf{R}, \tag{8}$$

where $\boldsymbol{\Lambda}_\mathrm{Q} \in \mathbb{C}^{N_\mathrm{C},N_\mathrm{C}}$ denotes a correlation matrix that models the channel and imperfections in compound with the inner

code. Then, the outer code $\mathbf{R}$ can be optimized to achieve the best-possible diversity gain by maximizing the pairwise product distance [11]. If $\mathbf{\Lambda}_{\mathrm{Q}}$ is a diagonal or quasi-diagonal matrix, the already employed outer code can be further used. The additional ISI that is introduced by TO and multipath propagation is compensated by an appropriate decoder, whereas the same receiver as for the initial design can be reused. Because LSDCs already employ a random phase inner code $\ddot{\mathbf{C}}_{\mathrm{TX,i}}$ [2], it is nearby to model the impact of multiple CFO, i. e. an additional phase shift per symbol, in compound with $\ddot{\mathbf{C}}_{\mathrm{TX,i}}$. Thus, inherent code properties of LSDCs are utilized emphasizing the advantages of those compared to other STBCs which underlines the proposal from [2].

To determine $\mathbf{\Lambda}_{\mathrm{Q}}$, we employ a matrix $\mathbf{Q} \in \mathbb{C}^{N_{\mathrm{C}}+N_{\mathrm{taps}}+\tau_{\mathrm{i}}-1,N_{\mathrm{C}}}$ that describes the transmit behaviour or respectively properties for all links and that can be obtained by a superposition of each links' property matrix $\mathbf{Q}_{\mathrm{TX,i}} \in \mathbb{C}^{N_{\mathrm{C}}+N_{\mathrm{taps}}+\tau_{\mathrm{i}}-1,N_{\mathrm{C}}}$, so that $\mathbf{\Lambda}_{\mathrm{Q}} = \mathbf{Q}^H \cdot \mathbf{Q}$, whereas $\mathbf{Q} = \sum_{i=1}^{N_{\mathrm{TX}}} \mathbf{Q}_{\mathrm{TX,i}}$.

$\mathbf{Q}_{\mathrm{TX,i}}$ summarizes the transmit properties for the link between the i-th TX and RX. It can be composed as

$$\mathbf{Q}_{\mathrm{TX,i}} = \ddot{\mathbf{\Phi}}_{\mathrm{TX,i}} \cdot \mathbf{\Theta}_{\mathrm{TX,i}} \cdot \mathbf{H}_{\mathrm{TX,i}} \cdot \ddot{\mathbf{C}}_{\mathrm{TX,i}} \tag{9}$$

$$= \ddot{\mathbf{\Phi}}_{\mathrm{TX,i}} \cdot \mathbf{H}^{\Theta}_{\mathrm{TX,i}} \cdot \ddot{\mathbf{C}}_{\mathrm{TX,i}}. \tag{10}$$

Thereby, $\mathbf{\Theta}_{\mathrm{TX,i}} \in \mathbb{C}^{N_{\mathrm{C}}+\tau_{\mathrm{i}}+N_{\mathrm{taps}}-1,N_{\mathrm{C}}+N_{\mathrm{taps}}-1}$ indicates a delay matrix, i. e. an identity matrix whose rows are shifted according to the link specific TO τ_{i}. E. g. $\mathbf{\Theta}_{\mathrm{TX,i}}\,(\tau_{\mathrm{i}} = 2)$ for $N_{\mathrm{C}} = 4$ and $N_{\mathrm{taps}} = 2$ is

$$\mathbf{\Theta}_{\mathrm{TX,i}}\,(\tau_{\mathrm{i}} = 2) = \begin{pmatrix} 0 & 0 & 0 & 0 & 0 \\ 0 & 0 & 0 & 0 & 0 \\ 1 & 0 & 0 & 0 & 0 \\ 0 & 1 & 0 & 0 & 0 \\ 0 & 0 & 1 & 0 & 0 \\ 0 & 0 & 0 & 1 & 0 \\ 0 & 0 & 0 & 0 & 1 \end{pmatrix}. \tag{11}$$

Without any TO and multipath propagation, each transmit property matrix is a diagonal matrix. However, in presence of aforementioned impairments the overall transmit property matrix $\mathbf{Q}$ is no diagonal matrix anymore. ISI is introduced, represented by the non-zero, non-diagonal elements. $\mathbf{Q}$ is used to perform a matched multiplication, so that the matched received symbol vector $\mathbf{y}_{\mathrm{m}} \in \mathbb{C}^{N_{\mathrm{C}},N_{\mathrm{C}}}$ can be obtained by

$$\mathbf{y}_{\mathrm{m}} = \mathbf{R}^H \cdot \mathbf{Q}^H \cdot \mathbf{y}. \tag{12}$$

The corresponding correlation matrix $\mathbf{\Lambda} \in \mathbb{C}^{N_{\mathrm{C}},N_{\mathrm{C}}}$ immediately follows as

$$\mathbf{\Lambda} = \mathbf{R}^H \cdot \mathbf{Q}^H \cdot \mathbf{Q} \cdot \mathbf{R}. \tag{13}$$

$\mathbf{y}_{\mathrm{m}}$ and $\mathbf{\Lambda}$ are forwarded to a decoder, whereas it is important to denote, that our proposed equalizer structure is not limited to a specific one. In fact, the choice is arbitrary. Because the decoding complexity is majorly dominated by this selection, the overall complexity of our equalizer is in principle flexibly adaptable. An iterative decoder, e. g. a MAP-MMSE-DFE receiver [12], should be preferably used due to its enhanced capability to deal with interference compared to linear representatives. The mentioned MAP-MMSE-DFE in particular enables a flexible trade-off between the achievable performance and decoding complexity by varying the decision threshold.

The system model is summarized in Fig. 2. Compared to the initial design (see Fig. 3), the proposed equalizer structure (see Fig. 4) utilizes additional knowledge about the CFO and TO introduced by each link to mitigate the impact of these impairments. It is worth pointing out, that this structure considers multipath channels, denoted by a channel vector for each link ($\mathbf{h}_{\mathrm{i}}$), while the initial design is based on narrow-band channels, denoted by a single channel coefficient for each link (h_{i}).

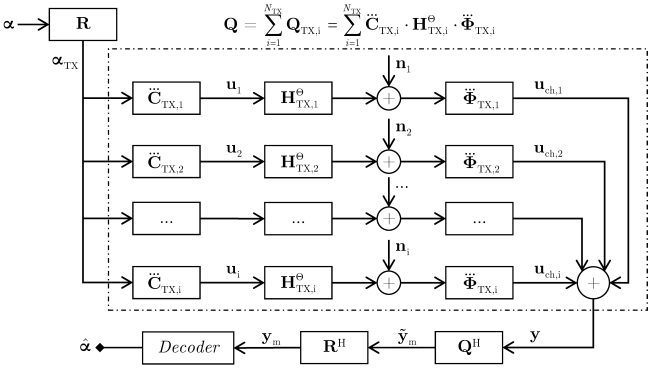

Fig. 2. Proposed System Model

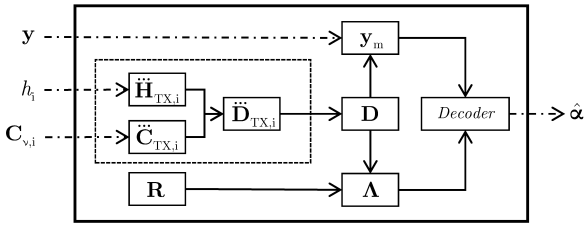

Fig. 3. Structure of the initial equalizer that neglects any impairments and presumes narrow-band channels

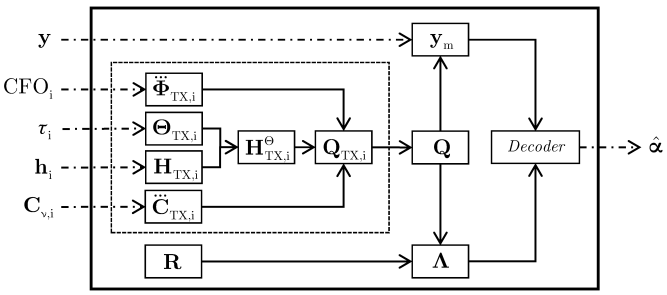

Fig. 4. Structure of the proposed equalizer that considers multiple TO, CFO and multipath propagation

A. Outer Code Considerations

The structure of $\mathbf{\Lambda}_{\mathrm{Q}}$ determines the necessary optimization for the outer code $\mathbf{R}$. $\mathbf{\Lambda}_{\mathrm{Q}}$ results mainly from the multiplication of diagonal matrices as

$$\mathbf{\Lambda}_{\mathrm{Q}} = \mathbf{Q}^H \cdot \mathbf{Q} \tag{14}$$

$$= \ddot{\mathbf{C}}^H_{\mathrm{TX,i}} \cdot \left(\mathbf{H}^{\Theta}_{\mathrm{TX,i}}\right)^H \cdot \ddot{\mathbf{\Phi}}^H_{\mathrm{TX,i}} \cdot \ddot{\mathbf{\Phi}}_{\mathrm{TX,i}} \cdot \mathbf{H}^{\Theta}_{\mathrm{TX,i}} \cdot \ddot{\mathbf{C}}_{\mathrm{TX,i}}. \tag{15}$$

Only $\mathbf{H}^{\Theta}_{\mathrm{TX,i}}$ and accordingly $\left(\mathbf{H}^{\Theta}_{\mathrm{TX,i}}\right)^H$ are no diagonal matrices. However, for a reasonable delay and N_{taps}, the structure is quasi-diagonal as all elements are located at the vicinity of the main diagonal, wherefore the initial outer code can be further used without any adaptations.

B. Fractional Delay

The proposed equalizer is immediately able to cope with fractional delays, i. e. delays equal to non-integer multiples of the symbol duration, if an upsampling is used. If SPS refers to the upsampling factor, i. e. the samples per symbol, fractional delays as integer multiples of $\frac{1}{\mathrm{SPS}}$ can be considered.

C. Concatenation of Blocks

For practical systems, typically several blocks are concatenated to a burst, while one block represents one encoded $\boldsymbol{\alpha}$. Then, TO and multipath propagation additionally cause an inter-block-interference (IBI). The information obtained at the receiver for preceding blocks ($\mathbf{Q}_{\mathrm{TX,i}}$ and $\hat{\boldsymbol{\alpha}}$) can be used to cancel IBI. However, IBI cancellation comes at the downside of lost information, as the delayed, i. e. overlapping elements of each block, cannot be used for decoding, so that the cancellation is limited to a reasonable delay and N_{paths}. For our simulations, we use a guard interval of appropriate length to decouple the impact of cancellation.

IV. Performance Comparison

Simulations are performed to verify that the proposed structure is able to retain the diversity performance with respect to the achievable bit error rate (BER) for a given energy per bit to noise ratio ($\frac{E_{\mathrm{b}}}{N_0}$). Within this section, we temporarily concentrate on a MANET setup with 4 TX and 1 RX. In Section V we consider larger, more realistic MANET setups. We assume Rayleigh fading channel coefficients and vary the number of channel taps N_{taps}, i. e. the distinctness of multipath propagation, as well as the timing and carrier frequency offset. We do not consider a power decay profile (PDP) for multipath propagation, so that each path has the same mean power. To avoid any SNR gain due to that, we scale each channel coefficient vector by $\sqrt{\frac{1}{N_{\mathrm{taps}}}}$.

The MANETs of interest are typically operated in the UHF-band, wherefore a carrier-frequency of $f_{\mathrm{c}} = 500$ MHz is presumed for the remaining. Besides, the simulations are based on a sampling time of $t_{\mathrm{s}} = 10$ μs. Limiting the simulations on oscillators with an accuracy of 100 ppm, the CFO is randomly varied between ± 50 kHz for each TX and transmission. We presume that the received signal spectrum is totally covered by the filter bandwidth, i. e. the CFO is bounded with respect to the receive filter. For transmit signal generation we use a rectangular pulse form filter.

Without loss of generality it can be assumed, that one signal is non-delayed, so that the delay of the remaining signals can be expressed relative to it. Simulations are performed according to "delay classes" τ which denote the maximum TO relative to a symbol duration that is regarded in the specific simulation run. E. g. the delay class $4T_{\mathrm{sym}}$ means that a maximum delay of $\tau = 4T_{\mathrm{sym}} = 4 \cdot \mathrm{SPS} \cdot t_{\mathrm{s}}$ is considered. Thereby, $\mathbf{u}_1$ is assumed to be non-delayed ($\tau_1 = 0$), while all other transmit signals are randomly delayed between $[0, +\tau]$.

With respect to the LSDCs, an outer code length of $N_{\mathrm{C}} = 32$ is selected as it has been shown to be a reasonable choice to achieve full transmit-diversity in combination with an iterative decoder [2]. The number of information symbols is chosen to match the outer code length ($N_{\mathrm{I}} = N_{\mathrm{C}} = 32$), so that rate one is attained ($R_{\mathrm{C}} = \frac{N_{\mathrm{I}}}{N_{\mathrm{C}}} = 1$). Unless explicitly mentioned, a numerically optimized cyclic matrix is employed as outer code that maximizes the minimum product distance [11], while a random phase matrix is used as inner code [2]. Thereby, a different random phase matrix is generated for each transmission. A 4-QAM is disposed as single-carrier scheme. Using a higher order modulation scheme is straightforward and does not require any changes to the proposed equalizer. Only the computational effort for an iterative decoding increases accordingly.

For all simulations an iterative MAP-MMSE-DFE receiver is employed, whereas the decoding error threshold is set to 0, so that only one symbol is decoded per iteration. It is presumed that the RX has perfect knowledge about the CFO and TO introduced by each TX and that the sampling is the same for all nodes. Besides, perfect channel state information is assumed. Regarding well-known parameter estimation approaches and presuming sufficiently long training sequences, these assumptions appear feasible. It is worth pointing out that there is no increase in the necessary effort or complexity as the parameter estimation has to be typically performed anyway similarly for all comparable communication systems.

Fig. 5 depicts the obtained results. The proposed scheme allows to effectively mitigate the impact of arbitrary multiple TO, CFO and multipath propagation. Regarding a specific multipath scenario, it can be stated, that the major diversity gain can be retained and is approximately the same despite the presence of comparably large TO and CFO. It attracts attention, that multipath propagation is highly beneficial. This is founded in the outer code structure, which is designed such that it allows to exploit additional degrees of freedom that the channel introduces. In fact, this has been one major reason, why we choose LSDCs as transmit diversity scheme and propose a tailored adapted equalizer for those. Comparing the results to that achievable with concurrent broadcasting (see Section V for explanation) and classical multi-hop communication, where only 1 TX is active at a time, highlights the advantages of cooperative transmission. The necessary $\frac{E_{\mathrm{b}}}{N_0}$ to undercut a certain BER level is significantly reduced.

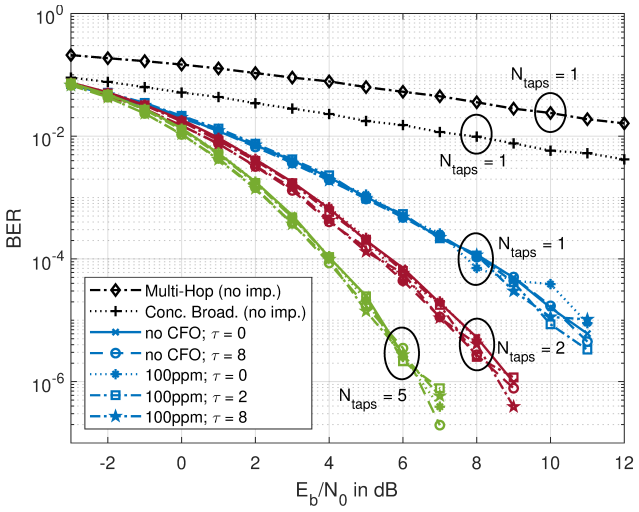

Fig. 5. Performance comparison: BER vs. $\frac{E_b}{N_0}$

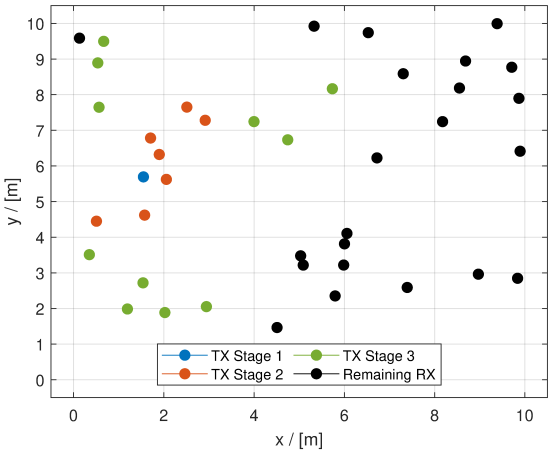

Fig. 6. Exemplarily propagation in a MANET if cooperative broadcasting is employed

V. MANET Simulations

Within this section, we study the effectiveness of our proposed decoder in a more realistic scenario with cooperative broadcasting. The latter is particularly suited to stress the achievements: In a cooperative setup, more and more nodes become active, that all induce a different CFO. Besides the distances, and thus the TO, become steadily larger. In brief, the considered impairments prominently emerge for each hop. To point out the benefits of cooperative broadcasting, we compare the results to classical multi-hop communication, where only 1 TX is active at a time, for which we choose non-cooperative flooding as a robust representative [2].

For the comparison, we assume that a varying number of nodes N_{nodes} is randomly distributed in an area of limited size (10×10 m). The totality of nodes composes a population. A two dimensional area is considered, so that all nodes are presumed to be at the same height. For cooperative broadcasting, one node starts to transmit a message. Surrounding nodes, that are able to successfully decode the packet, join transmission and support the broadcasting which is exemplarily shown in Fig. 6. By that, more and more nodes become active which typically increases the transmission range, so that the network can be covered with less hops. Employing a STBC allows to additionally profit from transmit diversity. All active TX simultanously transmit the same information, but a different transmit signal ($\mathbf{u}_1 \neq \mathbf{u}_2 \neq \ldots \mathbf{u}_{N_{TX}}$) which according to the STBC scheme add up in power and not in amplitude. In a concurrent broadcasting scenario, where all nodes send the same information and transmit signal, the signals add up in amplitude, so that destructive interference can occur.

A network is covered, i. e. the broadcast is successful, if all nodes can be reached. A node is considered to be reached if it is able to decode the message with a BER that is below 10^{-2}, while we choose latter, because common forward error correction (FEC) schemes typically allow to correct remaining bit errors once this threshold is undercut. For one random topology, we simulate various channel realizations and use the mean BER to decide which of the receiving nodes become TX for the next hop. Repeating this for several random topologies allows to determine an outage rate R_{out} as

$$R_{\text{out}} = \frac{N_{\text{out}}}{N_{\text{topo}}}, \tag{16}$$

where N_{out} denotes the number of failed broadcasts and N_{topo} the number of topologies. The algorithm is posed in Fig. 7. Every transmission between all active TX and each RX can

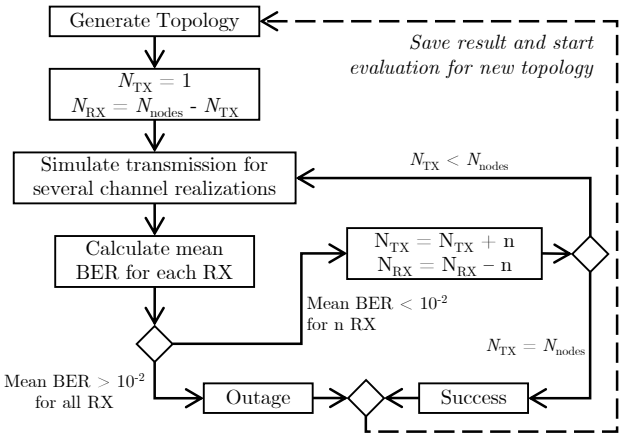

Fig. 7. Algorithm to detect outage / success in MANET simulations

be modelled as a virtual multiple-input single-output (MISO) setup (which corresponds to our simulations in Section IV), whereas a different multipath channel between each TX and RX is assumed that varies from hop to hop. Furthermore, a distance-dependent path-loss is considered. Hence, each channel coefficient is scaled with $\sqrt{d_i^{-\eta}}$, where d_i refers to the distance between the i-th TX to the appropriate RX and $\eta = 4$ to the path-loss coefficient of a suburban environment. While we vary the number of channel taps independently, the

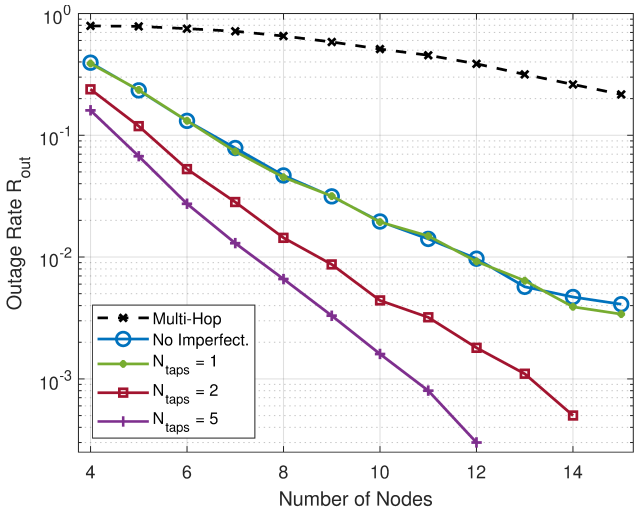

Fig. 8. Outage rate for varying population sizes

TO for the i-th link is determined with respect to the specific distance as

$$\tau_{\mathrm{i}} = \left\lceil 1\frac{\mathrm{sym}}{\mathrm{m}} \cdot (d_{\mathrm{i}} - d_{\mathrm{min}}) \right\rceil, \tag{17}$$

where d_{min} denotes the minimum distance between all active TX to the RX, i. e. refers to the earliest arriving signal and $\lceil \cdot \rceil$ to a ceil rounding operation. We arbitrarily choose $1\frac{\mathrm{sym}}{\mathrm{m}}$, so that a higher TO is introduced than actually expected due to the propagation for the given setup. However, this allows to study the principal robustness for an increased level of TO as it will be prevelant in an extended area. Additionally, each node introduces a different CFO. All nodes transmit with $E_{\mathrm{b}} = 1$, while the noise variance is $\sigma_{\mathrm{n}}^2 = 10^{-4}$.

Fig. 8 depicts the outage rate R_{out} with respect to a varying population size for non-cooperative multi-hop communication, cooperative broadcasting without any imperfections (one path, no TO and CFO) as well as cooperative broadcasting in presence of multiple TO and CFO, where N_{paths} is varied. The advantage of cooperative broadcasting compared to a non-cooperative multi-hop communication is clearly apparent. R_{out} is tremendously lower. Besides, our proposed scheme enables to effectively mitigate the imperfections, i. e. the performance can be retained. In fact, multipath propagation is advantageous as already reflected in Section IV, leading to an even further reduced outage rate. Cooperative broadcasting typically comes at the downside, that, at least for our simulations, more TX are active more often.

VI. Conclusion

We propose an effective equalizer structure that enables distributed cooperative transmission in MANETs with high node mobility when typical impairments are considered. The impact of arbitrary multiple CFO, TO and multipath propagation can be successfully mitigated. In fact, the proposed equalizer in combination with LSDCs profits from multipath propagation, i. e. frequency diversity, although the equalization is purely performed in the time-domain. Hence, neither a transformation nor a cyclic-prefix is required, which reduces the computational complexity and necessary overhead.

High node mobility, as prevelant in VANETs and FANETs [13], [14], causes frequent disconnections and topology changes. Common routing protocols rely on broadcasting topology control messages which limits the overall scalability [15]. We exemplary demonstrate the benefits in a broadcasting scenario and show by simulations, that cooperative broadcasting has a huge potential to improve the distribution of messages in a MANET which can therefore fructify in an improvement of the overall scalability.

Acknowledgment

This research work has been funded by *armasuisse Science and Technology*.

References

[1] A. Dusia and A. Sethi, "Software-defined architecture for infrastructure-less mobile ad hoc networks," in *2021 IFIP/IEEE Int. Symp. on Integrated Network Management (IM)*, pp. 742–747, 2021.

[2] M. Yüksel, R. Rolny, M. Kuhn, and M. Kuhn, "Applicability of space-time block codes for distributed cooperative broadcasting in manets with high node mobility," *IEEE 95th Vehicular Tech. Conf. VTC Spring*, 2022.

[3] M. Nahas, A. Saadani, and G.-B. Othman, "Bounded delay-tolerant space time codes with optimal rates for two cooperative antennas," in *21st Annual IEEE Int. Symp. on Personal, Indoor and Mobile Radio Com. (PIMRC)*, pp. 6–11, 2010.

[4] A. Desouky and A. El-Mahdy, "Asynchronous down-link cooperative communication scheme in rayleigh fading wireless environment," in *2016 Signal Processing: Algorithms, Architectures, Arrangements, and Applications (SPA)*, pp. 142–146, 2016.

[5] F. Alotaibi and J. Chambers, "Extended orthogonal space-time block coding scheme for asynchronous cooperative relay networks over frequency-selective channels," in *2010 IEEE 11th Int. Workshop on Signal Processing Advances in Wireless Com. (SPAWC)*, pp. 1–5, 2010.

[6] M. Damen and A. Hammons, "Delay-tolerant distributed-tast codes for cooperative diversity," *IEEE Transactions on Information Theory*, vol. 53, no. 10, pp. 3755–3773, 2007.

[7] A. Elazreg, U. Mannai, and J. Chambers, "Distributed cooperative space-time coding with parallel interference cancellation for asynchronous wireless relay networks," in *SoftCOM 2010, 18th Int. Conf. on Software, Telecommunications and Computer Networks*, pp. 360–364, 2010.

[8] M. Nahas, A. Saadani, and G.-B. Othman, "Bounded delay-tolerant space time block codes for asynchronous cooperative networks," *IEEE Transactions on Wireless Com.*, vol. 10, no. 10, pp. 3288–3297, 2011.

[9] Y. Liu, W. Zhang, and P. Ching, "Time-reversal space–time codes in asynchronous two-way relay networks," *IEEE Transactions on Wireless Com.*, vol. 15, no. 3, pp. 1729–1741, 2016.

[10] M. Nahas, A. Saadani, and R. Hatoum, "Asynchronous space time block codes: Low complexity decoding methods," in *2011 IEEE 12th Int. Workshop on Signal Processing Advances in Wireless Com.*, pp. 401–405, 2011.

[11] A. Wittneben and M. Kuhn, "A new concatenated linear high rate space-time block code," in *IEEE 55th Vehicular Tech. Conf. VTC Spring*, vol. 1, pp. 289–293, 2002.

[12] M. Kuhn and A. Wittneben, "A new scalable decoder for linear space-time block codes with intersymbol interference," in *IEEE 55th Vehicular Tech. Conf. VTC Spring*, vol. 4, pp. 1795–1799, 2002.

[13] H. Saleh and S. Hasson, "A survey of routing algorithms in vehicular networks," in *2019 Int. Conf. on Advanced Science and Engineering (ICOASE)*, pp. 159–164, 2019.

[14] J. Lin, W. Cai, S. Zhang, X. Fan, S. Guo, and J. Dai, "A survey of flying ad-hoc networks: Characteristics and challenges," in *2018 Eighth Int. Conf. on Instrumentation Measurement, Computer, Communication and Control (IMCCC)*, pp. 766–771, 2018.

[15] G. Kaur and P. Thakur, "Routing protocols in manet: An overview," in *2019 2nd Int. Conf. on Intelligent Computing, Instrumentation and Control Technologies (ICICICT)*, vol. 1, pp. 935–941, 2019.